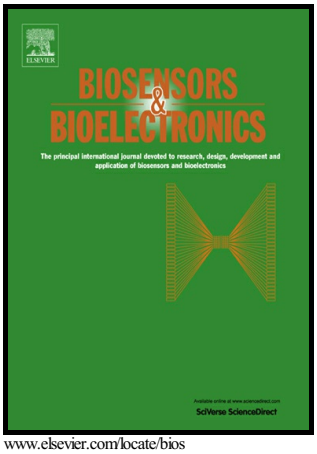

www.elsevier.com/locate/bios

A novel immunosensor based on excessively tilted fiber grating coated with gold nanospheres improves the detection limit of Newcastle disease virus

Binbin Luo, Yangfei Xu, Shengxi Wu, Mingfu Zhao, Pengjun Jiang, Shenghui Shi, Zhonghao Zhang, Yin Wang, Linlin Wang, Yong Liu

PII: S0956-5663(17)30606-1
DOI: http://dx.doi.org/10.1016/j.bios.2017.08.064
Reference: BIOS9974

To appear in: *Biosensors and Bioelectronic*

Received date: 27 June 2017
Revised date: 18 August 2017
Accepted date: 30 August 2017

Cite this article as: Binbin Luo, Yangfei Xu, Shengxi Wu, Mingfu Zhao, Pengjun Jiang, Shenghui Shi, Zhonghao Zhang, Yin Wang, Linlin Wang and Yong Liu, A novel immunosensor based on excessively tilted fiber grating coated with gold nanospheres improves the detection limit of Newcastle disease virus, *Biosensors and Bioelectronic,* http://dx.doi.org/10.1016/j.bios.2017.08.064

A novel immunosensor based on excessively tilted fiber grating coated with gold nanospheres improves the detection limit of Newcastle disease virus

Binbin Luo[a,c], Yangfei Xu[a], Shengxi Wu[b*], Mingfu Zhao[a], Pengjun Jiang[b], Shenghui Shi[a], Zhonghao Zhang[b], Yin Wang[a], Linlin Wang[b], Yong Liu[c]

[a]Chongqing Key Laboratory of Optical Fiber Sensor and Photoelectric Detection, Chongqing University of Technology, Chongqing 400054, China

[b]School of Pharmacy and Bioengineering, Chongqing University of Technology, Chongqing 400054, China

[c]School of Opto-electronic Information, University of Electronic Science and Technology of China, Chengdu 610054, China

[*]Corresponding author. sxwu2004@cqut.edu.cn

http://dx.doi.org/10.1016/j.bios.2017.07.100 0956-5663/& 2017 Elsevier B.V.

ABSTRACT

A novel immunosensor for detecting Newcastle disease virus (NDV) was developed using excessively tilted fiber grating (Ex-TFG) coated with gold nanospheres (AuNs). AuNs were coated on the Ex-TFG surface via Au-S bonds using 3-mercaptopropyltrimethoxysilane (MPTMS), and the activated staphylococcal protein A (SPA) was linked to AuNs by covalent bonds via cysteamine. AuNs greatly enhanced the impact of the analyte on the fiber cladding mode through the local surface Plasmon resonance (LSPR) effect, thus improving the detection limit and sensitivity of the immunosensor. Meanwhile, SPA enhanced the bioactivity of anti-NDV monoclonal antibodies (MAbs), thus promoting the effectiveness of specific binding events on the fiber surface. Immunoassays were performed by monitoring the resonance wavelength shift of the proposed sensor under NDV samples containing different particle amounts. Specificity was assessed, and clinical tests for NDV were performed by contrast experiments. Experimental results showed that the detection limit for NDV was about 5~10 times improved compared to that of reference Ex-TFG without AuN treatment. Moreover, the novel biosensor was reusable and could potentially be applied in clinic.

Keywords: Excessively tilted fiber grating (Ex-TFG); New castle disease virus (NDV); immunosensor; Au nanospheres (AuNs); Staphylococcal protein A (SPA)

1. Introduction

Thanks to advantages such as compact structure, wavelength modulation, fast detection, and remote sensing, many optical fiber grating types, including cladding-etched fiber Bragg grating (FBG), long period fiber grating (LPFG), and tilted fiber Bragg grating (TFBG), are widely applied in biochemical fields, e.g. drug characterization, food security, medical detection and diagnosis, environmental monitoring and virus detection (Krishnendu et al., 2016; Jörg et al., 2015; Albert et al., 2013). Meanwhile, with the biomolecular affinity of gold/gold nanoparticles and unique optical property of supporting surface Plasmon resonance (SPR) or localized SPR (LSPR), optical fiber (OF) based SPR/LSPR biosensors attract increasing attention (Kim et al., 2013; Ahmmed et al., 2016). Shao et al. (2010) reported that TFBG sensors with a tilted angle of ~10° excite SPR at a wavelength of ~1550 nm by coating the fiber surface with a ~50 nm thick gold film, thus greatly improving the refractive index (RI) sensitivity. From then on, Au/Ag coated TFBG-SPR sensors have been developed for many bio-sensing applications, such as high resolution aptasensor (Albert et al., 2013), real-time analysis of cellular behavior (Shevchenko et al., 2014), small biomolecule immunosensing (Ribaut et al., 2016), cancer biomarker detection (Ribaut et al., 2017) and highly sensitive detection of urinary protein (Guo et al., 2016) etc. However, the best detection limits of them for the corresponding targets could only reach the magnitude of sub-nM scale, e.g. 0.4nM for cytokeratin 7 peptide detection (Ribaut et al., 2016).

Compared to OF-SPR biosensors, OF-LSPR variants are much more localized, allowing for probing at the platform interface with spatial sensitivities well within the nanometer scale (Piliarik et al., 2012). Bialiayeu et al. (2012) showed that TFBG modified with metal nanoparticles can also excite LSPR at a wavelength of ~1.55μm. Lepinay et al. (2014) analyzed TFBG modified with several types of gold nanoparticles for protein detection, with greatly improved detection limit to be 8 pM for the case of gold nanocages.

Previously, we developed label-free immunosensors based on excessively tilted fiber gratings (Ex-TFGs) immobilized with specific monoclonal antibodies (MAbs) via staphylococcal protein A (SPA), for specific and fast detection of porcine circovirus type 2 (PCV2) (Luo et al., 2016) and heart failure (HF) biomarkers (Luo et al., 2017). Unlike TFBGs with small tilted angles (≤~20°), the excessively tilted finings (~81°) in Ex-TFGs can couple the core mode to higher-order co-propagating cladding modes, making it resemble LPFG (Shu et al., 2002) but with a relatively smaller grating period (Zhou et al., 2006). Combined with the large birefringent effect induced by the excessively tilted structure, Ex-TFGs have the advantages of negligible thermal cross-talk effect, higher RI sensitivity, and higher Q-factor compared with conventional LPFG based biosensors (Yan et al., 2015). However, in our previous studies, the Ex-TFG based PCV2 immunosensor could only achieve a detection limit of 9.371 $TCID_{50}$/mL (Luo et al., 2016), and the Ex-TFG based HF biomarker one only ~0.5ng/mL (Luo et al., 2017). Therefore, the detection limit of Ex-TFGs, as biochemical platforms, for viruses or biomarkers remains not satisfactory.

In this work, based on the previous SPA-modified method, a gold nanosphere (AuN) coated Ex-TFG to construct a novel type of immunosensor, which to be our best knowledge has not been reported, for the label-free, high specificity, ultra-trace and fast detection of Newcastle disease virus (NDV). NDV, a highly infectious chook disease induced by the NDV strain (Alexander et al., 2001; Sanchez et al., 2016), is wildly distributed in countries around the world, due to high transmission rate, with high mortality. Currently, with the application of several methods for NDV detection, e.g. chicken embryo inoculation(Chen et al., 2015), serological assays such as hemagglutination inhibition (HA-HI) test, serum neutralization and enzyme linked immunosorbent assay (ELISA)(Swain et al., 1999), as well as molecular diagnostic techniques, including reverse transcription polymerase chain reaction (RT-PCR) (Qiu et al., 2014) , monoclonal antibody method (Sun et al., 2010) and gene chip (Zhao et al., 2015), the spread of NDV has been effectively controlled to some extent.

However, these purely biochemical methods are somewhat limited. Chicken embryo inoculation is sensitive and specific (Roy et al., 2000), but the whole process requires about 3 weeks, and the operation is complex, which is not conducive for on-site detection. The HA-HI test is also sensitive, but the result might be significantly affected by external factors, which reduces the practical value of this method. ELISA is suitable for large-scale serological studies(Das et al.,2015), but it also has disadvantages including long time consumption, low specificity, complex process, and inconvenient on-site operation. Although the PCR test possesses high sensitivity as it directly identifies viral genes(Desingu et al., 2015), the high cost in equipment still restricts the use of this method in clinical practice. Therefore, developing detection alternatives is very important for the effective prevention and control of NDV.

The NDV immunosensor proposed in this study was constructed through several surface modified steps in a sequence that include silanization of the Ex-TFG by 3-mercaptopropyltrimethoxysilane (MPTMS), linkage of AuNs to MPTMS, SPA absorption, and immobilization of home-made highly purified anti-NDV MAbs. NDV immunoassay experiments were conducted in vitro by monitoring the resonance wavelength shift of the AuN modified Ex-TFG under NDV samples containing different particle amounts. For comparison, NDV detection by a reference Ex-TFG without AuN treatment was also performed. Reusability of the proposed Ex-TFG immunosensor was realized by a designed elution mechanism; finally, specificity assessment and clinical tests for NDV were performed by contrast experiments.

2.Materials and methods

2.1 Reagents

Analytical grade reagents and sterile deionized water were used for all working solutions. 3-Aminopropyltriethoxysilane (APTES), highly purified SPA, fluorescein isothiocyanate (FITC), 1-ethyl-3-[3-dimethylaminopropyl]carbodiimide hydrochloride (EDC), N-Hydroxysuccinimide (NHS), Tris, glycine, cysteamine, polyethylene glycol (PEG-1500), hypoxanthine-aminopterin-thymidine (HAT) and hypoxanthine-thymidine (HT) supplemented medium were purchased from Sigma-Aldrich, China. Phosphate buffered solution (PBS) (0.01 M, pH7.4) and 4-morpholineethanesulfonic acid hydrate (MES) (0.1 M, pH5.5~6.7) buffered solution were obtained from Wuhan Boster Biological Technology, China. AuNs (~80 nm) were purchased from Nanjing Nanoeast Biological Technology, China, and MPTMS was from Damas-beta, Switzerland. Protein A and G chromatography media were purchased from GE, USA. The NDV-AV29 strain was purchased from China Institute of Veterinary Drug Control; the H5 avian influenza virus strain was a kind gift from the Department of Veterinary, Nanjing Agricultural University. To prepare the NDV allantoic fluid, SPF chick embryos (aged 9 d) were inoculated with diluted NDV-AV29 (0.2 mL) into the allantoic cavity. The eggs were hatched at 37^{o}C for 48h, followed by allantoic fluid collection. The avian influenza virus (AIV) allantoic fluid was prepared in the same way as the NDV allantoic fluid.

2.2 Fabrication of Ex-TFGs and experimental setup

The scanning amplitude mask technique and doubled frequency Ar+ laser (244 nm) were used for the fabrication of Ex-TFGs, as comprehensively described by Zhou et al. (2006). The fabricated Ex-TFGs had a tilted angle of ~81° in the fiber core with a grating period of ~32.0 μm along the fiber axis (Fig. S1(a) and (b)) and a grating length of 10 mm. Since the fabrication process is highly standardized, Ex-TFGs are cost effective, easily made and reproducible. The transmission principle and sensing properties of Ex-TFGs have been specifically elaborated by Yan, et al. (2016). Usually speaking, the angle of Ex-TFG could be design and fabricated between 78.5°~83°, in which impaction of the tilt angle on the RI and temperature sensitivity of the sensor could be neglected. While the main factor to influence the RI and temperature sensitivity of the sensor is the cladding-mode order. Therefore, in order to guarantee the high-order cladding mode to appear in C/L-band to achieve a relatively high RI sensitivity by the constraint condition of grating period ~32μm, we choose the tilt angle to be 81°. In this case, the corresponding cladding-mode order of the grating is 32nd and 31st in the C and L band, respectively (Yan et al., 2016). The RI and temperature sensitivities of the cladding-mode resonance of the Ex-TFGs used in this study were ~180 nm/RIU (RI 1.33~1.38) and ~5 pm/°C, respectively.

Fig. 1 shows the experimental setup for monitoring the transmission spectrum of the Ex-TFG sensor. Broadband light from one output of the fiber optical grating demodulation system (FOGDS) (MOI-SM125, wavelength accuracy ±1 pm), integrated with a sweep laser light source (1510~1590 nm, 1Hz), was launched into the SM28 fiber. The isolator was used to cut off the backscattering and reflected light. The inline polarizer and polarization controller (PC) were used to excite and maintain light launching into the Ex-TFG to allow function in TM mode resonance (Fig. S2), since the SPR/LSPR effect can only be excited by the fiber's TM mode (Allsop et al., 2007). The Ex-TFG sensor was fixed in the biochemical reaction vessel when we carried out the immunoassay. Finally, the transmission spectrum was recorded by another channel of the FOGDS.

2.3 Preparation and identification of the anti-NDV MAbs

BALB/c mice were immunized four times with the inactivated purified subtype AV29 NDV, and spleen cells and SP2/0 cells were fused with PEG-1500 to prepare murine anti-NDV MAbs. A cell fusion rate of 94.0% was obtained, an indirect ELISA was developed to detect the MAbs secreted by hybridoma cell lines. A positive rate of 30.5% was obtained. One hybridoma cell line secreting MAbs to NDV, named 13E7, was developed into two subclones. After purification by Protein A affinity chromatography (Fig. S3(a)), 16 mg anti-NDV MAbs with 96.8% purity at a concentration of 1.938 mg/mL were obtained (Fig. S3(b)). The specificity of anti-NDV MAbs was assessed by Western-blot (Fig. S3(c)). The prepared anti-NDV MAbs would be very useful for the diagnosis and control of Newcastle disease.

2.4 Modification of the surface of Ex-TFGs

In this study, two Ex-TFGs with approximately the same RI sensitivity underwent surface modification. The first, labeled 'Ex-TFG1' was modified with AuNs, while the other, termed 'Ex-TFG2', without AuN treatment was used as a reference sensor for comparison.

Initially, these two Ex-TFGs were immersed in HNO_3 solution (5% v/v) for ~2h at ~40°C to remove the contamination, and thoroughly washed with deionized water and ethanol. The cleaned Ex-TFGs were immersed in the H_2SO_4 solution (95% v/v in H_2O_2) for ~1h at room temperature followed by drying in a convection oven for ~16h at 80°C. This step was performed to activate hydroxyl groups ('–OH') on the fiber surface.

EDC (4 mg/mL) and NHS (7 mg/mL) solutions were added to the prepared SPA solution (1 mg/mL in MES, pH 6.0) for 15min to activate the carboxyl groups ('–COOH') of SPA. Then, the activated SPA solution was diluted to 0.3 mg/mL by MES, and the pH adjusted to 7.2 before use.

Immersion of Ex-TFG1 was performed in the MPTMS solution (1% v/v in glacial acetic acid) followed by incubation in a convection oven for ~12 min at 80°C and air drying. The hydrosulphonyl groups ('–SH') of MPTMS would be exposed on the fiber surface. Washing was carried out with absolute

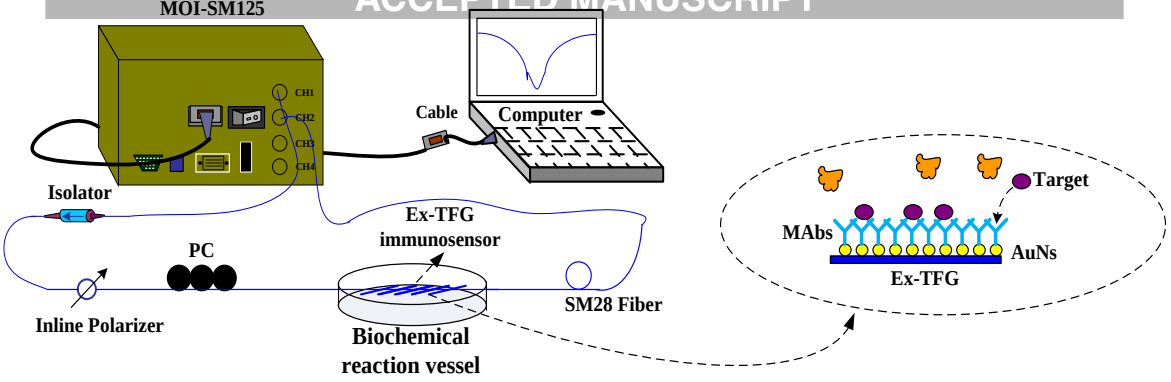

Fig. 1. Experimental setup for monitoring the transmission spectrum of the Ex-TFG immunosensor. (Inset: Immunoreaction scheme on the fiber surface)

ethanol and de-ionized water to thoroughly remove unbound silane compounds. Next, we immersed the samples in the 80 nm AuN solution for 12h at room temperature, during which AuNs would bind to MPTMS on the fiber surface through 'Au-S' bonds (Zhang et al., 2012). Then, PBS was used for multiple washing steps to remove unbound AuNs. The AuNs-immobilized Ex-TFG was immersed in the cysteamine solution (0.5 mM in ultrapure water) for 1h (room temperature), during which cysteamine was bound to the AuNs on the fiber surface by 'Au-S' bonds, with the amino groups ('$–NH_2$') exposed on the fiber surface. Subsequently, we immersed the samples in the activated SPA solution (300μL, 0.3 mg/mL) for ~40 min at room temperature, and SPA's –COOH could covalently bind to the cysteamine's $–NH_2$, thus producing a firm SPA molecular film on the fiber surface. Finally, the Ex-TFG1 was incubated in the highly purified anti-NDV-MAb solution (0.1835 mg/mL in PBS, 0.3 mL) for 1h at room temperature, and thoroughly washed with PBS to remove unbound anti-NDV MAbs. The whole chemical binding mechanism of anti-NDV MAbs to the Ex-TFG1 surface is depicted in Fig. 2.

The reference immunosensor (i.e. Ex-TFG2) was built through several steps in a sequence that included silanization by the APTES solution, covalent binding of the SPA layer, and immobilization of highly purified anti-NDV MAbs. The surface modification method for Ex-TFG2 was similar to that previously used for PCV2 and HF immunosensors (Luo et al., 2016; Luo et al., 2017), with the only difference that the MAbs used in this study were highly purified anti-NDV MAbs. The whole chemical binding mechanism of anti-NDV MAbs to the Ex-TFG2 surface is shown in Fig. S4.

3. Results and Discussion

3.1 Identification of the surface modification of Ex-TFGs

Spectra of Ex-TFG1 and Ex-TFG2 immersed in blank PBS (0.01M, pH7.4) were recorded after every step of the surface modification. As shown in Fig. 3(a) and (b) (first surface modification), wavelength shifts of Ex-TFG1 were ~0.765, ~0.68, ~0.275, ~0.375 and ~0.19 nm due to adsorption of MPTMS, AuNs, cysteamine, SPA and anti-NDV MAbs, compared to the previous modification step, respectively. By applied the RI sensitivity of ~180nm/RIU and the wavelength shift of every modified step in Fig. 3(a), the RI of the MPTMS, AuNs, cysteamine, SPA and anti-NDV MAbs layer could be estimated to be 1.33755, 1.34132, 1.34285, 1.34493 and 1.34599, respectively. For Ex-TFG2, wavelength shifts were ~0.385, ~0.255 and ~0.21 nm due to adsorption of APTES, SPA and anti-NDV MAbs, respectively (Fig. S5). Because the additional layer on the fiber surface affects the effective RI of cladding modes, altering the core-to-cladding coupling resonance conditions, the spectrum changes are reasonable, and suggested that the expected layers have been successively added on the fiber surface after each modification step.

A field emission scanning electron microscope (SEM) (ZEISS SIGMA HD) was used to assess the coating consistency of MPTMS and AuNs on Ex-TFG1. As shown in Fig. 4(a) and (b), surface modification was evident, indicating that the process used for silanization and the subsequent AuN modification yielded uniform and nicely adherent layers. Fig. 4(b) also shows that AuNs were evenly distributed on the fiber surface, which a more clear SEM image (44.11 k ×) of the AuNs on Ex-TFG1 is shown in Fig. S6(a).

Furthermore, the energy spectrum diagram and the corresponding percentage mass content for the Ex-TFG1 surface after AuN modification were also assessed (Fig. S6(b) and Table S1). The weight percentages of Au and S contents were 0.24% and 0.11%, respectively, with 'Au' and 'S' representing elements of the 'Au-S' bond between AuNs and the MPTMS layer.

To provide a visible image of the SPA layer coated on the fiber surface, several bare single-mode fibers were also submitted to the same modification process with Ex-TFG1 and Ex-TFG2, respectively. We used a prepared FITC-labeled-SPA solution (0.05 mg/mL in PBS with 1% BSA), which was activated by EDC/NHS chemistry, for the SPA-modification steps. Then, FITC-labeled-SPA treated fibers were observed under an inverted fluorescence microscope (Olympus Venox). Fig. 4(c) and Fig. S7(a) show fluorescence images of the FITC-labeled-SPA modified fibers with and without AuN treatment, respectively. Both of them show strong glowing fluorescence, giving fairly good evidence to the consistent SPA layer established on the fiber surface.

As control experiments, fibers only modified by MPTMS or APTES were also assessed under the same conditions. As shown in Fig. S7(b), no fluorescence was observed. Therefore, fluorescence (Fig. 4(c) and Fig. S7(a)) would be attributed to the presence of SPA molecular layer adsorbed on the fiber surface. The above findings demonstrate that the processes used for the immobilization of SPA molecules on the Ex-TFG1 and Ex-TFG2 surfaces are effective.

3.2 NDV detection by Ex-TFG1 and Ex-TFG2 immunosensors

First, the Ex-TFG1 was used for the assays. PBS was introduced in the

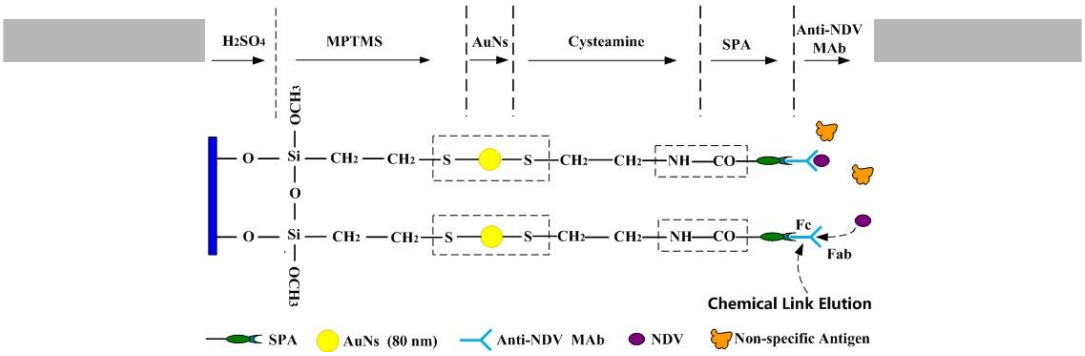

Fig. 2. Chemical binding mechanism on the Ex-TFG1 surface.

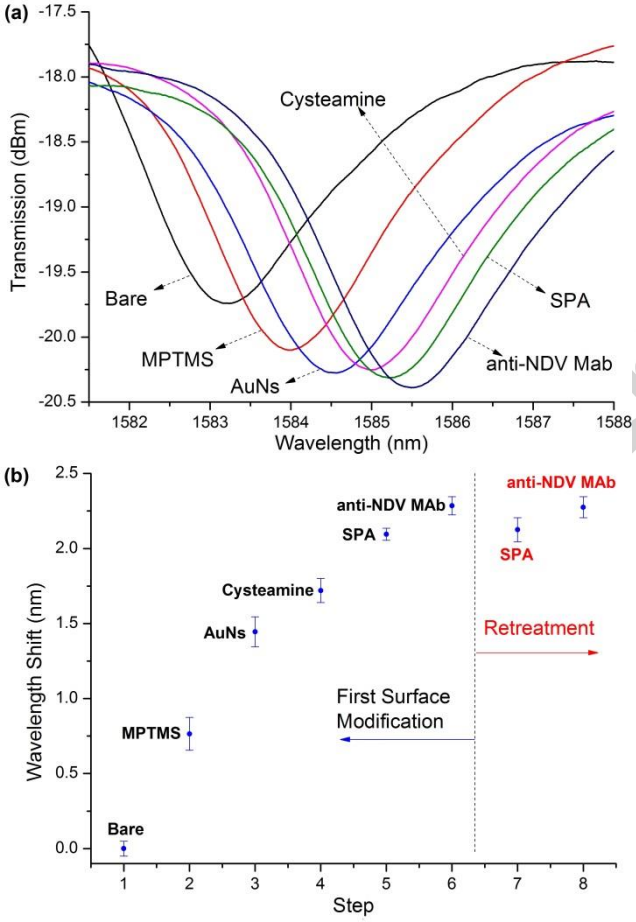

Fig. 3. (a) Spectrum evolution of the surface modification of Ex-TFG1; (b) resonance wavelength shifts of the first surface modification and subsequent ones.

biochemical reaction vessel, and the observed resonance wavelength was recorded as the reference. Subsequently, the prepared NDV samples (200μL) of different concentration (5, 10, 25, 50, 100, 200, 400, 800, 1000, 2400 and 5000 pg/mL) were used for immunoassay in turn. Spectrum changes were monitored online at each concentration level, with the spectrum recorded when it became stable.

The results showed that with increasing NDV concentrations, the time for the spectrum to become stable increased from ~5 min to ~25 min. This is reasonable because higher NDV concentrations would allow more NDV to be engages in the immunoreaction, thus leading to a longer reaction time.

The spectrum changes of Ex-TFG1 as NDV levels varied from 0 pg/mL to 1000 pg/mL are shown in Fig. 5(a), with corresponding resonance wavelength shifts (NDV levels of 0~5000 pg/mL) in Fig. 5(b).

According to Fig. 5(a) and (b), resonance wavelength was nearly unchanged between NDV concentrations of 5 pg/mL and 10 pg/mL; however, for a concentration of 25 pg/mL, an overt wavelength shift of ~75 pm was observed (inset in Fig. 5(b)). Because the temperature sensitivity of the Ex-TFG sensor is only ~5 pm/°C, which is a very small value. In this study, the immunoassay was carried out in lab at room temperature (25 °C) with fluctuation of ±0.5 °C, so even if temperature changes appear (1 °C or so), the influence on sensor response could be ignored. Therefore, the detection limit of Ex-TFG1 for NDV detection was estimated to be around 25 pg/mL.

Considering the NDV fusion protein molecular weight of 60KD (Fig. S3(c)), the detection limit could be convert into ~0.42 pM, which is better than that (0.4 nM) of TFBG-SPR biosensor for cytokeratin 7 peptide detection (Ribaut et al., 2016) and that (8 pM) of gold nanocages modified TFBG-LSPR biosensor for protein detection (Lepinay et al., 2014). However, at concentrations ≥~1000 pg/mL, the red-shift became saturated (~500 pm); indeed, the available Fab fragments of anti-NDV MAbs on the fiber surface were gradually enclosed by NDV as the virus amounts increased.

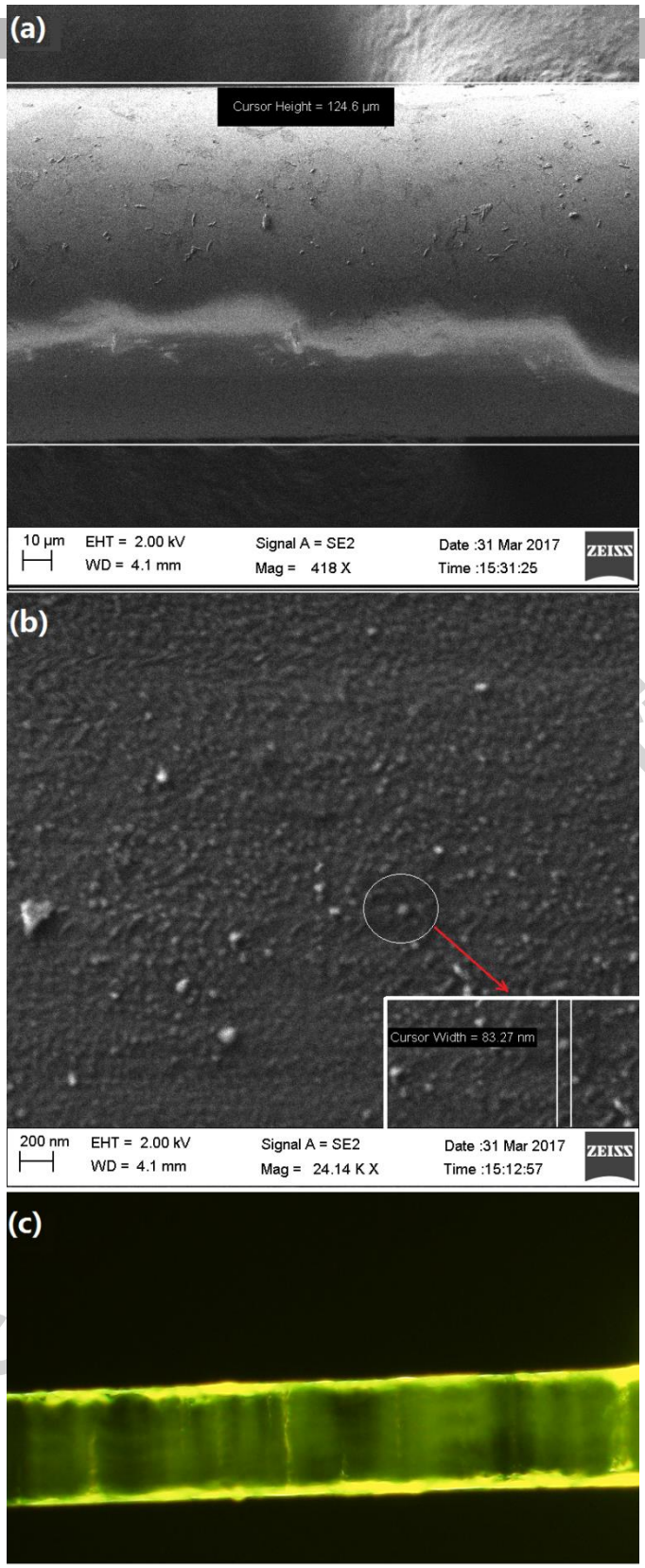

Fig. 4. SEM images of the surface configuration of (a) MPTMS (418 ×) and (b) AuN modified fibers (24.14 k ×). (c) Fluorescent image of FITC-labeled-SPA modified fibers with AuN treatment obtained by inverted fluorescence microscopy.

For comparison, Ex-TFG2 was used for the immunoassay with NDV concentrations of 50, 100, 200, 600, 1000 and 24000 pg/mL, respectively; the results in Fig. S8 indicated that the wavelength was nearly unchanged at a concentration of 50 pg/mL, but red shifts of ~20 pm and ~45 pm were obtained at 100 pg/mL and 200 pg/mL, respectively. Considering measurement errors, the detection limit of Ex-TFG2 for NDV was estimated

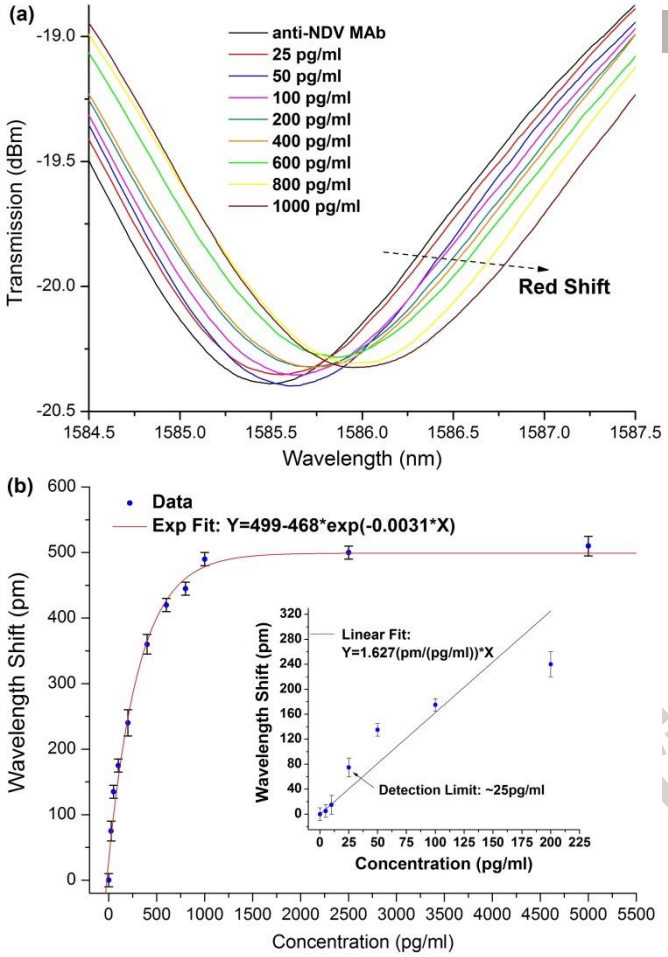

Fig. 5. (a) Spectrum evolution of Ex-TFG1 for NDV detection, and (b) corresponding resonance wavelength shifts and experimental fit for NDV concentrations of 0~5×10^3 pg/mL (Inset: Linear fit for NDV concentrations of 0~ 200 pg/mL).

to be between 100 pg/mL and 200 pg/mL. Therefore, the detection limit (~25pg/ml) of Ex-TFG1 was around 5~10 times improved compared to that of Ex-TFG2.

By using linear fit for a concentration range from 0 pg/ml to 200 pg/ml, the sensitivity of the Ex-TFG1 immunosensor was calculated to be ~1.627 pm/(pg/mL) (inset in Fig. 5(b)), i.e. ~10 times larger than that (~0.167 pm/(pg/mL)) of the reference value (inset in Fig. S8). In addition, saturated points of the Ex-TFG1 and the reference immunosensor were nearly the same (~1000 pg/mL), but the wavelength shift (~500 pm) at the saturated point for the former was ~1.7 time larger than that obtained for the latter (~300 pm). These results suggested that the available amounts of the Fab fragment on the Ex-TFG1 and reference surfaces are basically the same, but the sensitivity of the former remained better than that of the latter in the whole detection range (i. e. 0~1000 pg/mL).

The above advantages of the Ex-TFG1 immunosensor could be attributed to several factors, e.g. AuN treatment can magnify the effects of surrounding RI changes on the core to co-propagating cladding mode resonance of Ex-TFG through the intrinsic LSPR effect of AuNs, the combined effects of the bimolecular affinity of AuNs and the ability of SPA to enhance specific binding between anti-NDV MAbs and NDV; therefore, these factors greatly increase the detection limit and sensitivity of the proposed immunosensor**.**

3.3 Reusability assessment of the Ex-TFG1 immunosensor

Before evaluating the specificity and clinical performance of the proposed immunosensor, Ex-TFG1 was immersed in a pre-configured affinity balance solution (20 mM Tris-HCl, 150 mM NaCl, pH7.3-7.5) for 3 times, and 1 to 2 minutes for each time, and washed by affinity eluent (0.2 M Gly-HCl, pH3.0-3.2) for 6~7 times, and rinsed with affinity renewable solution (5.8 mL/L acetic anhydride, pH3.0) for 3~5 times.

The spectrum of the reprocessed Ex-TFG1 was recorded in PBS, and the resonance wavelength basically blue shifted back to that observed at the SPA-modification step (Fig. 3, Retreatment). These results indicated that anti-NDV MAbs were nearly removed from the fiber surface, while the SPA layer remained firmly attached thanks to covalent bonds to the fiber surface (Fig. 2).

Elution of anti-NDV MAbs from the SPA layer on the fiber surface is based on the chemical mechanism that low pH values could change the distribution of charges on the surface of conjugates, and repulsion between two like charges would cause them to separate; in the Gly-HCl buffer system, antibodies are more likely to aggregate and precipitate, thereby helping achieve the goal of separation.

The reprocessed Ex-TFG1 was incubated in the highly purified anti-NDV-MAb solution (0.1835 mg/mL in PBS, 0.3 mL) for 1h (room temperature) once again, and washed thoroughly with PBS. The recorded resonance wavelength red shift was ~0.15 nm (Fig. 3, Retreatment), confirming that the new anti-NDV MAbs were immobilized on the fiber surface. Therefore, the method used here for eluting anti-NDV MAbs from the SPA layer is efficient, and would constitute a good way for reusing the proposed immunosensor.

3.4 Specificity and clinical tests of the Ex-TFG1 immunosensor

Specificity assessment and clinical tests were carried out by using the reprocessed Ex-TFG1 immunosensor to analyze the home-made AIV, NDV-blank, and NDV allantoic fluids, successively.

In every test, Ex-TFG1 was immersed in the corresponding allantoic fluid (0.3 mL) for ~30 min followed by thorough wash with blank PBS, and the corresponding spectrum was recorded. Wavelength shifts are shown in Fig. 6, with the resonance wavelength of the anti-NDV-MAb re-immobilization step considered the reference point. Fig. 6 indicated that the sensor showed no response for the AIV and NDV-blank allantoic fluids, but exhibited an overt wavelength red-shift (~400 pm) for the NDV allantoic fluid.

Since these home-made allantoic fluids contained many biomolecular impurities, such as impure proteins, biological salts and cells, and SPA molecules are capable of binding many other anti-virus antibodies, these results suggested not only that the proposed Ex-TFG1 immunosensor is highly specific to NDV antigens and could be potentially applied in clinic, but also that activated SPA molecules exposed on the fiber surface have been totally enclosed by the Fc fragments of anti-NDV MAbs.

However, compared the results of Fig.6 and Fig.5(b), we could see that the wavelength red-shift (~400 pm) of Ex-TFG1 in the test for NDV allantoic fluid is lower than that (~500 pm) at the saturated point when it was used for the pure NDV solution test. These would be explained by two aspects. On

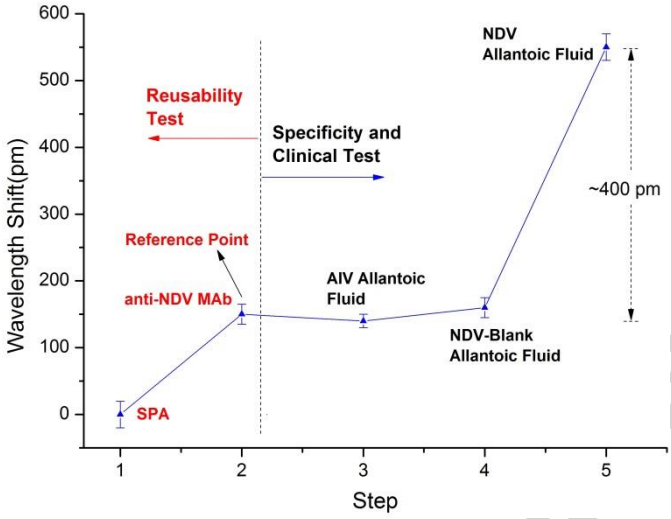

Fig. 6. Wavelength shift for reusability and specificity assessment, and clinical assay of the Ex-TFG1 immunosensor.

one hand, the specific antigen in allantoic fluid is the whole NDV virus, while for the purified solution test, it is highly purified NDV antigen protein, thus resulting the deference in the sensor response; on the other hand , as the sensor retreated by the home-made eluted fluids, the activity of SPA molecules attached on fiber surface would be degenerated by the chemical process , thus leading to the slide in the wavelength red-shift.

The above explanations are reasonable because in the following sequence, the Ex-TFG1 continue to be underwent the same chemical elution process and then the repeated test for the same NDV allantoic fluid for several times, and the results showed that the wavelength red-shift of Ex-TFG1 gradually downgraded as the increase of the repeat number.

4. Conclusions

We developed a novel immunosensor for fast and label-free detection of NDV based on Ex-TFG coated with AuNs (~80 nm). Due to the combined effects of AuN treatment and the SPA modification methodology, the detection limit and sensitivity of the proposed immunosensor are greatly enhanced compared with reference values. The immunosensor method established in this study had a minimum detectable virus concentration of ~25 pg/mL with a minimum detectable volume of 200 μL, thus its minimum detectable amount for NDV is ~5 pg. Therefore, the sensitivity of our method is slightly better than that of the most recently reported RT-PCR (10 pg) method (Ming et al., 2015). Besides, this method provides simple operation, requires shorter detection time, and does not need expensive reagents or equipment. Using a home-made elution mechanism to treat the fiber surface and conducting pre-designed control experiments, reusability, excellent specificity to NDV, and the potential clinical application of the proposed Ex-TFG immunosensor were demonstrated. Future research will focus on the impacts of structural parameters, e.g. fiber core/cladding diameter, and AuN shape (such as star-shape, nanorod, nanocage and nonocell) and diameter, on the performance of the proposed Ex-TFG immunosensor.

Acknowledgements

We acknowledge support from research funds of the National Natural Science Foundation of China (61505017, 61327004 and 61421002), the Foundation and cutting-edge Research Projects of Chongqing City (cstc2014jcyjA0081 and cstc2015jcyjA40035), China Postdoctoral Science Foundation(2016M592649), the Science and Technology Research Program of Chongqing Municipal Education Commission (KJ1709192 and KJ1709211), the Project Supported by Achievement Transfer Program of Institutions of Higher Education in Chongqing (KJZH14212), the Innovative Research Team Development Program in University of Chongqing (CXTDX201601031), and the Postgraduate Innovation Fund of Chongqing University of Technology (YCX2016103 and YCX2016242).

References

Krishnendu, D., Saurabh, M. T., Yasser, C., Wojtek, J. B., Predrag, M.,. 2016. Opt. Letters 41(18), 4198-4201.

Jörg, B., Amin, F., Wolfgang, S. and Björn, M.,. 2015. Opt. Letters 40(4), 546-549.

Albert, J., Shao, L.Y., Caucheteur, C., 2013. Laser and Photonics Reviews 7(1), 83-108.

Kim, J.A., Hwang, T., Dugasani, S.,R., Amin, R., Kulkarni, A., 2013. Sensors and Actuators B: Chemical, 187(4), 426-433.

Ahmmed, A. R., Mahdiraji, G. A., Yong, M., S., Rajib, A., Shee, Y. G., Mahamd, A., F., 2016. Opt. Express 24(3), 2485-2495.

Shao, L., Shevchenko, Y., Albert, J., 2010. Opt. Express 18(11), 11464-11471.

Albert, J., Lepinay, S., Caucheteur, C., DeRosa M. C., 2013, Methods 63, 239-254.
Shevchenko, Y., Camci-Unal, G., Cuttica, Davide, F., Dokmeci, Mehmet, R., Albert, J., Khademhosseini, Ali., 2014. Biosensors and Bioelectronics 56, 359-367.
Ribaut, C., Voisin, V., Malachovská, V., Dubois, V., Mégret, P., Wattiez, R., Caucheteur., C., 2016, Biosensors and Bioelectronics 77, 315-322.
Ribaut, C., Loyez, M., Larrieu., J., Chevineau, S., Lambert, P., Remmelink, M., Wattiez, R., Caucheteur., C., 2017, Biosensors and Bioelectronics 92, 449-456.
Guo, T., Liu F., Liang, X., Qiu, X., Huang Y., Xie, C., Xu, P., Mao W., Guan, B., Albert, J. , 2016, Biosensors and Bioelectronics 78, 221-228,.
Bialiayeu, A., Bottomley, A., Prezgot, D., Ianoul, A., Albert, J., 2012. Nanotechnology 23(44), 1607-1653.
Piliarik, M., Ŝípová, H., Kvasnička, P., Galler,N., Krenn,J.R., Homola,J., 2012. Optics Express 20(1),672-680.
Lepinay, S., Staff, A., Ianoul, A., Albert, J., 2014. Biosensors and Bioelectronics 52, 337-344.
Luo, B., Wu, S., Zou. W., Zhang, Z., Zhao, M., Shi, S., Liu, Y., Xi, X., Zeng, Z., Liang ,W., Yan, Zhi., Zhang, L., 2016. Biosensors and Bioelectronics 86, 1054-1060.
Luo, B., Wu, S., Zhang, Z., Zou. W., Shi, S., Zhao, M., Zhong, N., Liu, Y., Zou, X., Wang, L., Chai, W., Hu, C., Zhang, L., 2017. Biomedical optics express 8(1), 57-67.
Shu, X., Zhang, L., Bennion I., 2002, Journal of Lightwave Technology, 20(2),255-266.
Yan, Z., Wang, H., Wang, C., Sun, Z., Yin, G., Zhou, K., Wang, Y., Zhao, W., Zhang, L.,2016, Optics Express 24(11),12107-12115.
Alexander, D., Gordon, M. L., 2001, British Poultry Science 42(1),5-22.
Sanchez, D., Pelayo, R., Medina, L., Vadillo, E., Sánchez, R., Núñez, L., Cesarman, G., Sarmiento, R.,. 2016, Viruses 8(1), 3.
Chen, X., Li, Z., Hu, G., Gu S., Zhang S., Ying Y., Gao F.,2015, Avian Dis,59(2), 235-243.
Swain, P., Verma, K., Kataria, J., Mohanty S.,1999,Indian Journal of Experimental Biology 37(10), 1037-1038.
Qiu, X., Yu, Y., Yu, S., Zhang, Y., Wei, N., Song, C., Sun, Y., Tan, L., Ding, C., 2014, Scientific World Journal 2014(8), 934851.
Sun, Y., Chen, H., Song, C., Yu, Y., Qiu, X., Yu, S., Ding, C., 2010, Chinese journal of cellular and molecular immunology 5,464-466.
Zhao, Y., Huang, N., Wen, Y., Hu, Z., Yang, G., Ma, R., Hu, X., Zhang, X., Chang, X., Cao, S., Huang, X., Wu, R., Wen X., 2015, Chinese Journal of Veterinary Science 9,952-958.
Roy, P., Venugopalan, A.T., Koteeswaran, A., 2000, Trop Anim Health Prod 32(3):183-188
Das, M., Kumar, S., 2015, J Virol Methods 225:64–69
Desingu, P.A., Singh, S.D., Dhama, K., Vinodh, O,R., Singh, R.,Singh, R.K., 2015, J Virol Methods 212:47–52.
Zhou, K., Zhang, L., Chen, X., Bennion, I., 2006, Opt. Letters 31(9),1193-1195.
Allsop, T., Neal, R., Rehman, S., Webb, D. J., Mapps, D., Bennion, I., 2007, Applied Optics 46(22), 5456-5460.
Zhang, Q., Xue, C., Yuan, Y., Lee, J., Sun, D., Xiong, J., 2012, Sensors 12, 2729-2741.
Ming, W., Yin, R., Xie, G., Xue, C., Wang, K., Yuan, Q., Ding, Z., 2015, Chinese Journal of Veterinary Science 35(7),1056-1059.

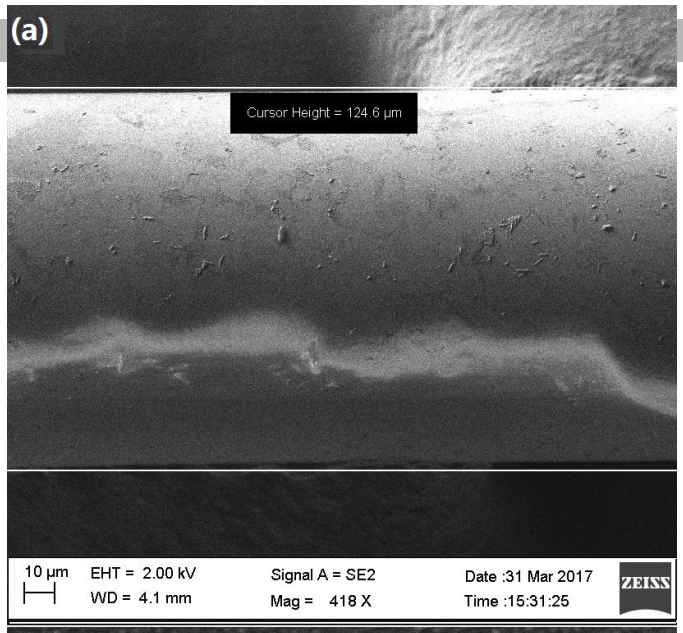
(a)
Cursor Height = 124.6 µm
10 µm
EHT = 2.00 kV
WD = 4.1 mm
Signal A = SE2
Mag = 418 X
Date :31 Mar 2017
Time :15:31:25
ZEISS

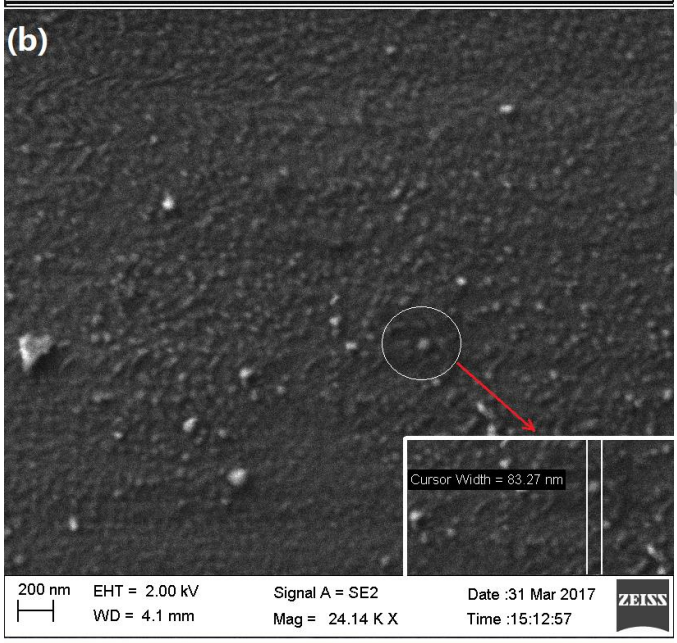
(b)
Cursor Width = 83.27 nm
200 nm
EHT = 2.00 kV
WD = 4.1 mm
Signal A = SE2
Mag = 24.14 K X
Date :31 Mar 2017
Time :15:12:57
ZEISS

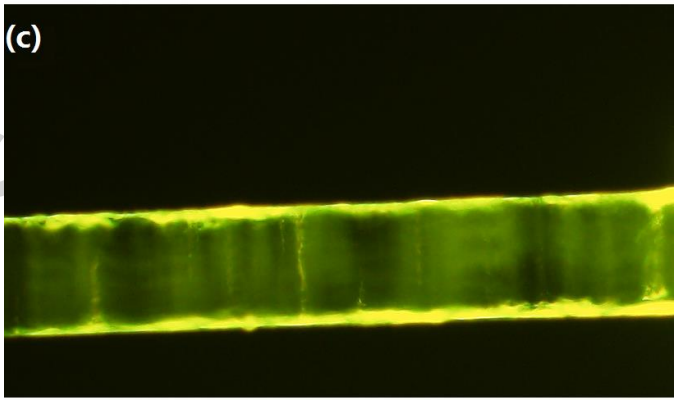
(c)